

Fine Control of the Release and Encapsulation of Fe Ions in Dendrimers through Ferritin-like Redox Switching

Reina Nakajima, Masanori Tsuruta, Masayoshi Higuchi, and Kimihisa Yamamoto*

Department of Chemistry, Faculty of Science and Technology, Keio University, Yokohama 223-8522, Japan

Received July 23, 2003; Revised Manuscript Received January 5, 2004; E-mail: yamamoto@chem.keio.ac.jp

Dendrimers having a uniform sphere-like structure are expected to have novel properties using the innervoids as “reaction flasks”¹ or “metal-storage capsules”² for nanoreaction chemistry. Recently, numerous dendrimers incorporating metal ions or clusters³ have received much attention as nanocatalysts and drug delivery materials⁴. We have already reported that tin ions, Sn²⁺ ions, are coordinated to the imine groups of a spherical phenylazomethine dendrimer (DPA) in a stepwise radial fashion, which should make it possible to control the number and location of the Sn ions incorporated into the dendrimers.⁵ We would like to expand the variety of metal ions that can be incorporated into DPA in a stepwise radial fashion to create novel organic-inorganic hybrid materials. As one of the most common and significant iron ions, Fe³⁺ was used for the incorporation into DPA. Iron possesses very interesting properties such as magnetism,⁶ redox chemistry,⁷ and catalysis⁸ and is also one of the essential elements of our body. There are some iron storage proteins called ferritins⁹ in the liver. The mechanism of encapsulation and release of iron is caused by the redox of the iron in the protein shell. Here, we show a successful attempt to control the “encapsulation/release” of iron ions in the dendrimer through the redox switching driven by the Fe²⁺/Fe³⁺ couple. This ferritin-like dendrimer is the first material that should prove to be useful for creating a drug delivery system.

DPA_s G0–G4 were synthesized using the convergent method through the dehydration of aromatic ketones with aromatic amines in the presence of titanium (IV) tetrachloride.^{5b} These imine groups act as strong coordination sites with the ferric ions. The fourth generation of dendritic polyphenylazomethine (DPA G4, Chart S1) having 30 imine groups should assemble 30 FeCl₃ molecules, because the imine group quantitatively complexes FeCl₃. During the addition of FeCl₃, the color of the chloroform/acetonitrile solution of DPA G4 changed from yellow to orange due to the complexation. Using UV–vis spectroscopy to monitor the titration until 30 equiv of FeCl₃ had been added, the absorption at λ_{max} = 410 nm increased without isosbestic points (Figure S1a). However, when subtracting the absorbance of FeCl₃ (ε_{Fe³⁺}[Fe³⁺]₀) possessing absorptions at λ_{max} = 310 and 360 nm from the spectra, we observed a decrease at the π–π* absorption of the imine bonds at 335 nm and four changes in the position of the isosbestic point, indicating that the complexation proceeds not randomly, but stepwise (Figure 1). These four shifts in the isosbestic points are similar to the complexation with SnCl₂. The spectra of DPA G4 gradually changed with an isosbestic point at 374 nm up to the addition of 2 equiv of FeCl₃. The isosbestic point then shifted during the further addition and appeared at 367 nm between 3 and 6 equiv. During the addition between 7 and 14 equiv of FeCl₃, an isosbestic point appeared at 365 nm and moved to 364 nm during the addition of between 15 and 30 equiv. The number of added equivalents of FeCl₃ that induced the shifts in the isosbestic points is in good agreement with the number of imine sites in each generation of DPA G4. This means that the complexing process proceeds in a stepwise fashion

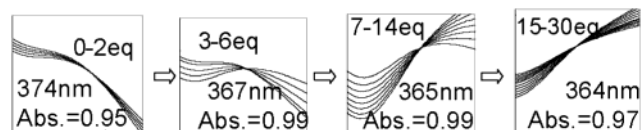
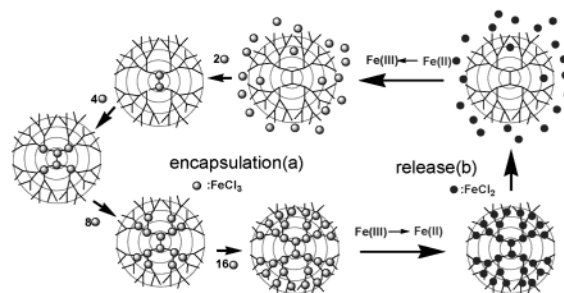


Figure 1. Isosbestic point changes in UV–vis spectroscopy during the addition of FeCl₃ to DPA G4 in CH₃CN/CHCl₃ = 1/1.

Scheme 1. Stepwise Radial Complexation of FeCl₃ and DPA G4(a), and Ferritin-like Redox Switching of Fe Ion’s Encapsulation(a)/Release(b) in DPA



from the core imines to the terminal imines of DPA G4 (Scheme 1a). A similar stepwise radial complexation was also observed in both DPA G2 and DPA G3. After subtraction of the absorption of FeCl₃, in the case of DPA G2, two isosbestic points appeared at 348 and 357 nm for the addition of 0–2 and 3–6 equiv of FeCl₃, respectively (Figure S2). For DPA G3, three isosbestic points also appeared at 375, 363, and 360 nm during the addition of 0–2, 3–6, and 7–14 equiv of FeCl₃, respectively (Figure S3). These results also support the idea that metal ions incorporate with DPA in a stepwise fashion, first filling the layer close to the dendrimer’s core and then progressively the more peripheral layers.

The C=N ligands usually make complexes with FeCl₃ and some crystal structures have been previously reported.¹⁰ As a control experiment, the complexation of FeCl₃ with the phenylazomethine dendrimer (DPA G0) that has one imine group was determined by UV–vis spectroscopy. During the titration with FeCl₃, the solution of DPA G0 changes from transparent to yellow. A Job plot in chloroform/acetonitrile (1/1) solvent (Figure S4) shows a maximum at a 0.5 mol fraction of DPA G0, i.e., DPA G0 is equimolecular with FeCl₃. This result supports the idea that the imine forms a 1:1 imine/FeCl₃ complex. The equilibrium constant of complexation, *K*, was determined to be ca. 10⁸ [M⁻¹], which is 100 times greater than that of SnCl₂ (cf. *K* = ca. 9.6 × 10⁵ M⁻¹), by curve-fitting a theoretical simulation to the experimental data.

Characterization of the DPA/FeCl₃ complex¹¹ was carried out by TOF-MS spectroscopy even though it is difficult to detect the molecular fragments because of the low ionization activity of the complex. The molecular fragments of (FeCl₃)₆@DPA G2 (calcd; 1153.49+6×162.21) were observed at 1153.8, 1317.5, 1481.6, 1645.3, 1807.8, and 1974.6 using a sample of the DPA G2 solution

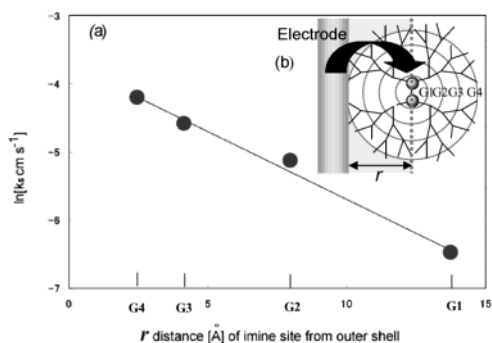


Figure 2. (a) Plots of $(\ln k_s)$ [cm s^{-1}]; electron-transfer rate constants of $(\text{FeCl}_3)_n$ @DPA G4 [$n = 2, 6, 14, 30$] vs distance r [Å] from outer shell to the imine site that complexes with FeCl_3 . The slope is -0.20 \AA^{-1} . (b) An image of the electron transfer through the shell of $(\text{FeCl}_3)_2$ @DPA G4.

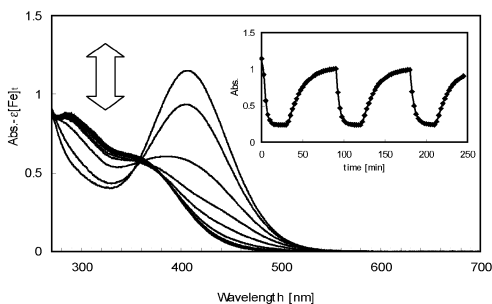


Figure 3. (a) Electro UV-vis spectra changes of $(\text{FeCl}_3)_{30}$ @DPA G4. $[\text{FeCl}_3] = 1 \text{ mM}$, $[\text{DPA G4}] = 33 \mu\text{M}$, $[\text{TBABF}_4] = 0.1 \text{ M}$, $+0.5 \text{ V}$ to -0.5 V vs Ag/Ag^+ . Working; Pt wire. (b) Absorption changes at 410 nm . The absorption change during the release is fitted to be first-order kinetics ($k = 4.2 \times 10^{-3} \text{ s}^{-1}$, $t_{1/2} = 2.75 \text{ min}$). Complexation is fitted to be second-order kinetics ($k = 1.42 \text{ s}^{-1} \text{ M}^{-1}$, $t_{1/2} = 11.7 \text{ min}$).

in which 6 mol equiv of FeCl_3 were added (Figure S5, Table S1). This result indicates that 3Cl^- and one imine of DPA are ligands of Fe^{3+} .

To confirm the radial stepwise complexation by another method, we employed an electrochemical analysis of the Fe ion redox in the dendrimer. The cyclic voltammetry of $(\text{FeCl}_3)_{30}$ @DPA G4 in chloroform/acetonitrile (1/1) solvent under an argon atmosphere shows the half-wave potential ($E_{1/2}$) of the $\text{Fe}^{2+}/\text{Fe}^{3+}$ couple at -0.28 V vs Fc/Fc^+ . However, in the case of $(\text{FeCl}_3)_2$ @DPA G4, an irreversible redox wave was observed (Figure S9). The electron-transfer rate of $(\text{FeCl}_3)_2$ @DPA G4 was determined to be $k_s = 0.0015 \text{ cm s}^{-1}$ which is much smaller than that of $(\text{FeCl}_3)_{30}$ @DPA G4 (0.015 cm s^{-1} , Table S2, Figure S10). We have already reported that DPAs were assembled on a substrate without deformation of the molecules because of the rigid structure.^{5b} In other words, the distance between the iron in the dendrimer and the electrode is maintained during the redox reaction. In the case of $(\text{FeCl}_3)_2$ @DPA G4, 2 Fe ions are coordinated to the imine groups near the core of DPA G4. The electron transfer is drastically suppressed because of the core-shell effect that iron ions complexed with the imine sites are separated from the electrode by more than ca. 1 nm. Furthermore, the distance from the outer shell to the Fe ions in DPA was estimated on the basis of the radial stepwise complexation fashion which could determine the precise location and number of metal ions. We first found the plot of $(\ln k_s)$ versus the distance¹² (Figure 2) to be linear in accordance with the Marcus theory.

The redox reaction of $(\text{FeCl}_3)_{30}$ @DPA G4 was also observed by spectroelectrochemical measurements. The time scale of the spectroelectrochemical measurement is 100 times larger than that

of CV. When the applied potential was changed from $+0.5 \text{ V}$ to -0.5 V to reduce Fe^{3+} , the absorption band around 410 nm , attributed to the complex, decreased, and then the spectra agreed with that of the DPA G4 without metals (Figure 3, ref Figure S1). FeCl_2 is not coordinated to DPA G0 due to the weak Lewis acidity ($K = \text{ca. } 0.8 \text{ M}^{-1}$, Figure S11). These results indicate that Fe ions are released from the dendrimers because of the drastic decrease in the equilibrium constants, K , attributed to the reduction of the Fe ions (Scheme 1b). It is reasonable to find a reversible assembly of Fe ions through electrooxidation, which allows the electrochemical switching of the encapsulation/release of Fe ions in the dendrimer like the iron storage protein, ferritin.

In summary, the assembly of the essential metal ions, FeCl_3 , in the DPA through the radial stepwise complexation, is electrochemically confirmed using $(\text{FeCl}_3)_2$ @DPA G4. It is possible to control the reversible encapsulation/release of Fe ions on the electrode. This study shows one of the steps to create a novel intelligent drug delivery system using highly organized material.

Acknowledgment. This work was partially supported by CREST from Japan Science and Technology Agency, Grants-in-Aid for Scientific Research (Nos. 15036262, 15655019, 15350073), and the 21st COE Program (Keio-LCC) from MEXT, and a Research Grant (Project No.23) from KAST.

Supporting Information Available: UV-vis spectra data, MS data, and additional data (PDF). This material is available free of charge via the Internet at <http://pubs.acs.org>.

References

- (1) (a) Jiang, D. L.; Aida, T. *Nature* **1997**, *388*, 454. (b) Kleij, A. W.; Gossage, R. A.; Klein Gebbink, R. J. M.; Brinkmann, N.; Reijerse, E. J.; Kragl, U.; Lutz, M.; Spek, A. L.; van Koten, G. *J. Am. Chem. Soc.* **2000**, *122*, 12112.
- (2) (a) Hecht, S.; Fréchet, J. M. *Angew. Chem., Int. Ed.* **2001**, *40*, 74. (b) Harth, E. M.; Hecht, S.; Helms, B.; Malmstrom, E. E.; Fréchet, J. M. J.; Hawker, C. J. *J. Am. Chem. Soc.* **2002**, *124*, 3926. (c) Newkome, G. R.; He, E.; Moorefield, C. N. *Chem. Rev.* **1999**, *99*, 1689.
- (3) (a) Zheng, J.; Dickson, R. M. *J. Am. Chem. Soc.* **2002**, *124*, 13982. (b) Zhao, M.; Crooks, R. M. *Adv. Mater.* **1999**, *11*, 217. (c) Lemon, B. I.; Crooks, R. M. *J. Am. Chem. Soc.* **2000**, *122*, 12886. (d) Scott, R. W. J.; Ye, H.; Henriquez, R. R.; Crooks, R. M. *Chem. Mater.* **2003**, *15*, 3873.
- (4) (a) Aoi, K.; Tsutsumiuchi, K.; Yamamoto, A.; Okada, M. *Tetrahedron* **1997**, *53*, 15415. (b) Crespo, L.; Sanclimens, G.; Montaner, B.; Perez-Tomas, R.; Royo, M.; Pons, M.; Albericio, F.; Giralt, E. *J. Am. Chem. Soc.* **2002**, *124*, 8876. (c) Stiriba, S. E.; Frey, H.; Haag, R. *Angew. Chem., Int. Ed.* **2002**, *41*, 1329. (d) Wiener, E. C.; Auteri, F. P.; Chen, J. W.; Brechbiel, M. W.; Gansow, O. A.; Schneider, D. S.; Belford, R. L.; Clarkon, R. B.; Lauterbur, P. C. *J. Am. Chem. Soc.* **1996**, *118*, 7774.
- (5) (a) Yamamoto, K.; Higuchi, M.; Shiki, S.; Tsuruta, M.; Chiba, H. *Nature* **2002**, *415*, 509. (b) Higuchi, M.; Shiki, S.; Ariga, K.; Yamamoto, K. *J. Am. Chem. Soc.* **2001**, *123*, 4414. (c) Imaoka, T.; Horiguchi, H.; Yamamoto, K. *J. Am. Chem. Soc.* **2003**, *125*, 340. (d) Satoh, N.; Cho, J. S.; Higuchi, M.; Yamamoto, K. *J. Am. Chem. Soc.* **2003**, *125*, 8104.
- (6) (a) Sun, S.; Zeng, H. *J. Am. Chem. Soc.* **2002**, *124*, 8204. (b) Rajamathi, M.; Ghosh, M.; Seshadri, R. *Chem. Commun.* **2002**, 1152.
- (7) (a) Daniel, M. C.; Ruiz, J.; Astruc, D. *J. Am. Chem. Soc.* **2003**, *125*, 1150. (b) Jeuken, L. J. C.; Jones, A. K.; Chapman, S. K.; Cecchini, G.; Armstrong, F. A. J. *J. Am. Chem. Soc.* **2002**, *124*, 5702.
- (8) (a) Choi, H. C.; Kim, W.; Wang, D.; Dai, H. *J. Phys. Chem. B.* **2002**, *106*, 12361. (b) Mayer, M. F.; M. Hossain, M. M. *J. Org. Chem.* **1998**, *63*, 6839.
- (9) (a) Kaim, W.; Schwederski, B. *Bioinorganic Chemistry: Inorganic Elements in the Chemistry of Life: An Introduction and Guide*; Wiley: England, 1994. (b) Zapfen, M. A.; Johnson, M. A. *J. Electroanal. Chem.* **2000**, *494*, 114.
- (10) (a) Cotton, S. A.; Franckevicius, V.; Fawcett, J. *Polyhedron* **2002**, *21*, 2055. (b) Drain, J. C.; Jeannin, Y.; Martin, L. M. *Inorg. Chem.* **1980**, *19*, 2935.
- (11) The exact masses of $(\text{FeCl}_3)_2$ @DPA G2 and $(\text{FeCl}_3)_2$ @DPA G3 were observed (Figure S6). Fragment peaks of $(\text{FeCl}_3)_n$ @DPA G2 ($n = 0, 2, 6$) were used as the confirmation of the radial stepwise complexation behavior (Figures S7, S8).
- (12) This time τ is determined by molecular modeling^{5b} of DPA G4 that was performed based on the crystal structure of DPA G2 on the basis that the size of DPA does not change during the complexation.

JA037480P